Hydrogen Bonding in Polymer-Solvent Mixtures

Ioannis G. Economou, Yuping Cui, and Marc D. Donohue*

Department of Chemical Engineering, The Johns Hopkins University, Baltimore, Maryland 21218

Received January 4, 1991; Revised Manuscript Received April 19, 1991

ABSTRACT: Hydrogen bonding between solvent molecules and between solvent and polymer molecules was investigated by FTIR spectroscopy. The solvents examined were compounds that can both self-associate and solvate (such as methanol) as well as compounds that can only solvate (such as tetrahydrofuran). Chloroform used as a cosolvent strongly solvates and there is spectroscopic evidence that it can weakly self-associate. The polymer used was a polyketone capable of solvating with molecules having acidic properties. Hydrogen bonding between an ether of moderate size and methanol also was examined. The extent of hydrogen bonding was determined by FTIR spectroscopy with a nonlinear regression technique. Chemical theory based on segment-segment interactions is used to model the spectroscopic results. Association between the different species is shown to be independent of the molecular size.

Introduction

Hydrogen-bonding complexes result from the interactions between a functional group capable of donating an electron and a group capable of accepting the electron. In general, polymer systems can solvate or self-associate depending on the functional groups of the polymer and solvent. For example, poly(ethylene glycol) can self-associate by forming hydrogen bonds between the hydroxyl end groups and the ether groups of the main chain. If there is an electron acceptor in the mixture, solvation complexes between this component and the ether groups of poly(ethylene glycol) also can be formed.

In this paper, we studied hydrogen-bonding interactions between small molecules as well as between solvent molecules and polymer sites using FTIR spectroscopy. The experimental data were modeled quantitatively by using chemical theory. Though hydrogen bonding in polymer systems has received considerable attention in recent years, this is the first work, as far as we know, where hydrogen bonding between small molecules and polymers is examined quantitatively using infrared (IR) spectroscopy. Philippova et al.[1] used IR spectroscopy to study the self-association of poly(ethylene glycol) in carbon tetrachloride. Equilibrium constants for the interactions between the hydroxyl end groups and the ether groups of the main chain were obtained. Coleman, Painter, and their co-workers[2-7] have performed extensive studies on hydrogen bonding in polymer blends using Fourier-transform infrared spectroscopy (FTIR). In their work, they examined exclusively hydrogen-bonding interactions among polymer molecules. In most of the blends examined, one of the polymers was capable of both self-association and solvation whereas the other polymer only was capable of cross-association (solvation). They also studied hydrogen bonds in an amorphous polyamide[6] and in a semicrystalline polyamide[7] using FTIR. Musto et al.[8] examined hydrogen bonding in polybenzimidazole-polyimide polymer blends using FTIR, and Allen et al.[9] measured heats of mixing and cloud point curves for mixtures of methoxylated poly(ethylene glycol) with methoxylated poly(propylene glycol).

Hydrogen bonding is very strong in aqueous polymer solutions. Water molecules self-associate forming three-dimensional clusters and they also solvate with polymer molecules having hydrogen-bonding groups. Hefford[11] examined the phase behavior of aqueous solutions of commonly used polymers such as dextran and poly(ethylene glycol). He calculated osmotic second virial coefficients and constructed phase diagrams for various aqueous polymer solutions. Haynes et al.[12] experimentally examined aqueous polymer solutions of poly(ethylene glycol) and dextran to obtain second and third osmotic viral coefficients. They also calculated liquid-liquid equilibria in ternary systems from the constituent binary mixtures. Diamond and Hsu[13] formulated a semiempirical thermodynamic expression based on the Flory-Huggins theory for the protein partitioning in poly(ethylene glycol)-dextran aqueous two-phase systems. Polik and Burchard,[14] using static light scattering, detected large aggregates of poly(ethylene oxide) in aqueous solutions. Courval and Gray[15] calculated values for the Flory-Huggins χ parameter for the same system using gas chromatography.

In this work, intermolecular hydrogen-bonding interactions between polymer sites and solvent molecules were examined experimentally by FTIR spectroscopy. Hydrogen bonding between small molecules also was determined. Our main interest was to examine the concentration and density dependence of the hydrogen bonding in polymer systems and to compare the results with results for small molecules. In addition, the effect of molecular size on hydrogen bonding was determined. Systems where noncompeting hydrogen bonding occurs and systems where more than one type of hydrogen-bonding complex is formed (competing systems) were examined. The monomeric and hydrogen-bonding peaks were recorded and analyzed by a nonlinear regression technique developed by Walsh et al.[16,17] This technique was used[17] to examine hydrogen-bonding competition in entrainer cosolvent mixtures. Chemical theory was used to model the specific interactions (hydrogen-bonding interactions) between polymer molecules and solvent molecules. This approach has been successful in modeling small molecules associating through Lewis acid-base interactions.[18] For the polymer mixtures site-site interactions are used rather than molecule-molecule interactions.

The good agreement between the experimental results and the theoretical model suggests that this approach can be used to improve phase equilibrium calculations for polymer systems.

* Author to whom correspondence should be addressed.

0024-9297/91/2224-5058$02.50/0

Table I
Systems Examined in This Work Using FTIR Spectroscopy[a]

solvent, mol_{seg}/L	cosolvent, mol_{seg}/L	solute, mol_{seg}/L
CCl_4	$CHCl_3$	THF
10.292	0.0	0.121
10.212	0.096	0.121
10.131	0.193	0.121
10.035	0.385	0.121
9.649	0.771	0.121
9.006	1.541	0.121
7.719	3.083	0.121
CCl_4	THF	CH_3OH
10.292	0.0	0.025
10.189	0.123	0.025
10.293	0.245	0.025
9.978	0.614	0.025
9.453	1.230	0.025
8.928	1.845	0.025
8.402	2.455	0.025
THF	$CHCl_3$	PVMK
12.286	0.0	0.05
12.132	0.154	0.05
11.979	0.309	0.05
11.672	0.617	0.05
11.057	1.233	0.05
9.829	2.466	0.05
8.600	3.699	0.05
7.372	4.932	0.05
THF	CH_3OH	PVMK
12.286	0.0	0.03
12.164	0.247	0.03
12.041	0.494	0.03
11.673	1.235	0.03
11.058	2.469	0.03
10.444	3.704	0.03
9.830	4.939	0.03
9.215	6.174	0.03
8.601	7.408	0.03
7.372	9.878	0.03
CCl_4	TGDE	CH_3OH
10.292	0.0	0.03
10.241	0.114	0.03
10.189	0.227	0.03
10.086	0.454	0.03
9.880	0.908	0.03
9.572	1.589	0.03
9.263	2.270	0.03
9.057	2.724	0.03
8.748	3.405	0.03
8.234	4.540	0.03

[a] CCl_4, carbon tetracloride; $CHCl_3$, chloroform; CH_3OH, methanol; PVMK, poly(vinyl methyl ketone); THF, tetrahydrofuran; TGDE, tetraethylene glycol dimethyl ether.

Experimental Procedure

In this work, a Mattson Polaris FTIR spectrophotometer with demountable cells with variable pathlength was used to record infrared spectra. All measurements were at 25 °C. In all systems examined, solute monomeric and hydrogen-bonded peaks were detected. Calculations were made by using the solute monomeric peak in the absence of any hydrogen-bonding interactions as a reference. The systems examined are shown in Table I.

Carbon tetrachloride (CCl_4) and methanol (CH_3OH) were from J. T. Baker Inc., and tetrahydrofuran (THF), poly(vinyl methyl ketone) (PVMK), chloroform ($CHCl_3$), and tetraethylene glycol dimethyl ether (TGDE) were from Aldrich Chemical Co. All liquid chemicals were stored under nitrogen. CCl_4 does not show hydrogen-bonding interactions, and it was used as an inert solvent for all the nonpolymer systems examined. $CHCl_3$ hydrogen bonds with basic molecules. In addition, there is spectroscopic evidence that it dimerizes weakly.[19,20] For the two polymer systems, THF was used as the solvent because it is a good solvent for the polymer examined (PVMK) and it does not hydrogen bond with it. CH_3OH was used both as a cosolvent and as a solute, whereas TGDE and PVMK were used only as solutes. TGDE is an ether with five oxygen atoms capable of donating electrons that can form from one up to five hydrogen bonds per molecule with electron acceptors. Its molecular structure is $CH_3(OCH_2CH_2)_4OCH_3$. It was used to examine the validity of our model for moderate molecular sizes. The polymer used (PVMK) is an electron donor with a carbonyl (C=O) group per segment, and its structure is $[-CH_2CH(COCH_3)-]_n$.

In all systems, the concentration of the solutes was constant and low and the concentration of the cosolvent varied from zero up to 20% (v/v). The concentration of the solutes was kept low so that their absorbance peaks would obey Beer's law and so that self-association (for methanol) would be prevented. For methanol concentration less than 0.03 mol/L, self-association of methanol can be ignored with no loss of accuracy.[17] In the CCl_4–$CHCl_3$–THF mixture, the THF concentration was 0.121 mol/L, in the CCl_4–THF–CH_3OH and in the CCl_4–TGDE–CH_3OH mixtures, the CH_3OH concentration was 0.025 and 0.03 mol/L, respectively, and in the THF–$CHCl_3$–PVMK and in the THF–CH_3OH–PVMK mixtures, the PVMK concentration was 0.05 and 0.03 mol_{seg}/L, respectively.

Data Analysis

The monomeric and hydrogen-bonded peaks of the solute were recorded and the areas of the peaks were determined by a nonlinear regression technique described in the Appendix. The concentration of the corresponding component is linearly related to the area of the peak according to Beer's law

$$A(\nu) = a(\nu)bC \tag{1}$$

where $A(\nu)$ is the area under the absorption peak at the wavenumber ν, $a(\nu)$ is the absorptivity of the peak, b is the path length, and C is the concentration of the sample. In this work, the absorption of the OH group of methanol at approximately 3650 cm^{-1} was examined for the systems where methanol was the solute. When methanol hydrogen bonds with another component in the solution, the resulting bonded peak of the OH group is well separated (at a lower frequency) from the nonbonded peak and it is different in shape so that quantitative analysis of the peak areas from the spectral data can be made. For the systems where PVMK was the solute, the C=O peak of the polyketone at approximately 1713 cm^{-1} was analyzed. When the carbonyl group of the polyketone hydrogen bonds, the bonded peak overlaps with the nonbonded peak. When this happens, it is difficult to get quantitative values for the peaks using only the raw spectra. Walsh et al.[16,17] developed a method to resolve the peaks using the Fourier self-deconvolution and first derivative of the spectral data. Limitations of this technique were discussed by Kauppinen et al.[21] The raw data, the first derivative of the data, and the Fourier self-deconvolution are fitted. Usually, a Lorentzian curve is used to fit spectral data. However, the Voigt profile has been shown to be better in fitting spectral data, and it was used for the data analysis in this work. The Voigt profile is given by the expression[22]

$$E(\nu,\nu_0,h,\alpha_L,\alpha_D) = h\frac{\ln 2}{\pi^{3/2}}\frac{\alpha_L}{\alpha_D^2}\int_{-\infty}^{+\infty}\frac{\exp(-t^2)}{\frac{\alpha_L^2}{\alpha_D^2}\ln 2 + \left[\frac{\nu-\nu_0}{\alpha_D}(\ln 2)^{1/2} - t\right]^2}\,dt \tag{2}$$

where ν is the wavenumber, ν_0 is the wavenumber at the peak maximum, h is the peak height, α_L is the Lorentzian half-width, and α_D is the Doppler half-width. A nonlinear regression technique was used to determine the four parameters (ν_0, h, α_L, α_D) for each peak, and the area under

the corresponding peak was calculated. A brief description of this technique is given in the Appendix.

Theoretical Framework

Since the pioneering work of Flory[23] and Prigogine,[24] many theoretical and semitheoretical equations of state have been developed to represent the thermodynamics of polymer solutions.[25-28] Group contribution methods have also been developed[29,30] in order to obtain generalized theories that would be applicable to small molecules as well as to polymers.

The description of the thermodynamic properties of polymer systems becomes more complicated for the systems where hydrogen-bonding interactions occur in addition to dispersion forces. Flory[31] was the first to propose a chemical equilibrium approach between the different species in a polymer mixture. This approach has been very successful for mixtures of small molecules (nonpolymers).[32] Tompa[33] provided a theoretical framework for treating associating species based on the quasichemical theory of Guggenheim. His work is strictly theoretical, and no attempt was made to obtain quantitative agreement with experimental data. Ginell and Shurgan[34] derived a linear association model for systems where one of the components self-associates. Renon and Prausnitz[35] and Wiehe and Bagley[36] used chemical theory to describe the vapor–liquid equilibrium and excess functions for mixtures of alcohols with hydrocarbons. In their analyses, they assumed infinite equilibria models for the alcohols and that the hydrocarbons did not self-associate or solvate.

To account for nonrandomness in polymer solutions due to hydrogen bonding, Renuncio and Prausnitz[37] presented a semiempirical equation based on Guggenheim's quasichemical theory which fitted mixing properties of binary polymer–solvent systems using two adjustable parameters. Similarly, Panayiotou and Vera,[38] starting from the quasichemical theory of Guggenheim, incorporated nonrandomness into the Flory equation of state[25] using expressions for local surfaces and local compositions. Calculations of the volumes and heats of mixing for solvent–polymer systems based on their equation are similar to the calculations using the Flory equation of state and are in good agreement with experimental data. However, the equation gives values for the χ parameter that are in better agreement with experimental values than other theories.

ten Brinke and Karasz[39] discussed the effect of directional-specific interactions (hydrogen bonding) on the LCST behavior of polymer blends. They showed that miscibility in polymer blends can be governed by the strength of the hydrogen bonding, by the difference in solubility parameters, and by the amount of entropy lost due to the formation of a favorable interaction. The compressibility of the mixture also is an important factor in determining miscibility. Recently, the model of ten Brinke and Karasz[39] was used in the lattice–fluid theory of Sanchez and Lacombe to take into account specific interactions and related entropic contributions.[40] In the modified Sanchez–Lacombe equation of state, the entropic interactions are temperature dependent. The model improved calculations of the spinodal phase diagram for the polymer blend of poly(vinyl methyl ether) and polystyrene. Prange et al.[41] formulated a semiempirical quasichemical partition function to represent the thermodynamic properties of aqueous solutions of linear polymers and cross-linked polymers, and they calculated VLE and LLE for different systems. In the partition function hydrogen bonding and dispersion interactions are taken into account explicitly and the exchange energies between the different sites are independent adjustable binary parameters.

Painter et al.[42-44] using chemical theory derived a thermodynamic model for polymer blends where one of the polymers self-associates through an infinite equilibria model and solvates to the second polymer. The second polymer does not self-associate but does form hydrogen bonds to the first. This approach is similar to the approach used in this paper. In their model, they calculate the Gibbs free energy of mixing from the Flory–Huggins expression by adding a term to account for the hydrogen-bonding interactions that is calculated through their chemical theory expressions. Theoretical phase behavior calculations were performed[45] and comparisons with experimental data were made.[46]

Chemical Theory for Polymer Systems

In all chemical theories it is assumed that when two molecules form a hydrogen bond, a new species is formed. In the special case where one of the two molecules is a polymer, one segment of the polymer reacts with one solvent molecule (which for simplicity here is assumed to be a small molecule) to form a new species according to the reaction

$$S + P \rightleftharpoons SP \tag{3}$$

where S denotes a solvent molecule, P denotes a polymer segment, and SP denotes a segment of the resulting species. Within this context, polymer molecules contain segments that are not hydrogen bonded (P segments) and segments that are solvated with a solvent molecule (SP segments). Following Flory,[31] we write the equilibrium constant in terms of molar concentrations as

$$K' = \frac{C_{SP}}{C_S C_P} \tag{4}$$

where C_i is the molar concentration of species i. The standard reference state of the molecular species is the state where the species are separated and oriented. The molar concentration of species i can be expressed in terms of the segment concentration of i if the number of segments per molecule is known

$$C_i^{seg} = C_i r_i \tag{5}$$

where r_i is the number of segments per molecule of i. In our analysis, we assume that the small solvent molecules consist of one segment per molecule and that solvation between a polymer segment and a solvent molecule does not increase the number of segments of the resulting polymer molecule. As a result, eq 4 can be expressed as

$$K' = \frac{C_{SP}^{seg}}{C_S^{seg} C_P^{seg}} \frac{r_P}{r_{SP}} = \frac{C_{SP}^{seg}}{C_S^{seg} C_P^{seg}} = K \tag{6}$$

By writing the equilibrium constant in terms of segment concentrations, we eliminate the complication caused by the fact that in a polymer molecule some of the sites are hydrogen bonded and the remaining sites are not. In the rest of this work, the equilibrium constant K in terms of segment concentrations is used exclusively. In addition, for simplicity in the notation we drop the superscript seg to denote segmental concentration. All concentrations hereafter are segmental concentrations except where stated otherwise.

Binary Mixtures. In a binary mixture where one of the components can donate electrons (a Lewis base) and

the other component can accept electrons (a Lewis acid) the following complex formation can occur

$$A + B \rightleftharpoons AB \tag{7}$$

where A denotes a segment of the Lewis acid molecule and B represents a segment of the Lewis base molecule. A and B can be either small molecules or polymers. The extent of hydrogen bonding for component B can be expressed as

$$\eta = \frac{C_{B_0} - C_B}{C_{B_0}} \tag{8}$$

where C_{B_0} is the superficial concentration of component B if no hydrogen bonding occurs and C_B is the non-hydrogen-bonding (or monomeric) concentration of component B. The notation C_{A_0} and C_A is defined similarly for component A. The equilibrium constant K_{AB} for eq 7 is

$$K_{AB} = \frac{C_{AB}}{C_A C_B} \tag{9}$$

The material balances for A and B are

$$C_{A_0} = C_A + C_{AB} = C_A(1 + K_{AB}C_B) \tag{10}$$

$$C_{B_0} = C_B + C_{AB} = C_B(1 + K_{AB}C_A) \tag{11}$$

Substituting eq 11 back into eq 8, one obtains

$$\eta = \frac{K_{AB}C_A}{1 + K_{AB}C_A} \tag{12}$$

From eqs 10 and 11 the following expression is obtained

$$C_{A_0} = C_A\left(1 + K_{AB}\frac{C_{B_0}}{1 + K_{AB}C_A}\right) \tag{13}$$

Solving the latter for C_A and substituting back into eq 12, one obtains an expression for η as a function of C_{A_0}, C_{B_0}, and K_{AB}.

In the case where component A self-associates in addition to the solvation between the two components, a second equilibrium constant is used to describe the self-association of A. In the case where A only dimerizes it is

$$A + A \rightleftharpoons A_2 \tag{14}$$

and

$$K_{AA} = C_{A_2}/C_A^2 \tag{15}$$

The material balance for component A is rearranged to account for the dimerization of A and it reads

$$C_{A_0} = C_A + 2C_{A_2} + C_{AB} = C_A(1 + 2K_{AA}C_A + K_{AB}C_B) \tag{16}$$

Substituting eq 11 into the latter, one obtains a cubic equation for C_A. Finally, η is calculated from eq 12.

Ternary Mixtures. For ternary mixtures where all three components can form hydrogen bonds the equations describing the chemical equilibria of the system are more complicated than in the case of the binary mixture,[18] and, to date, no analytical solution has been obtained. In this work, the ternary system studied consisted of a component A that can donate and accept electrons (an amphoteric component) and two components B and C that can only donate electrons (Lewis bases). Component A has two sites per segment capable of hydrogen bonding, and as a result it can form long i-mers according to the reaction

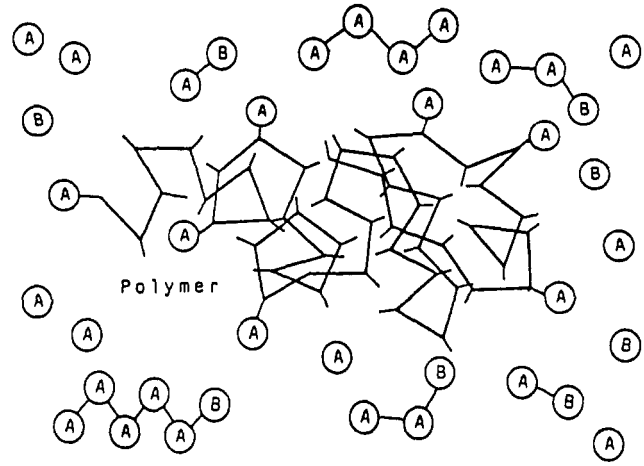

Figure 1. Schematic representation of the species existing in a ternary mixture of a component A that can self-associate and solvate with the other components, a component B that can only solvate with A and a polymer that has sites capable of forming hydrogen-bonding complexes with molecules of A.

$$A_i + A \rightleftharpoons A_{i+1} \tag{17}$$

where i can be an integer number from one to infinity. In addition, the acidic site of A can form a complex with either of the basic components B or C

$$A_i + B \rightleftharpoons A_iB \tag{18}$$

$$A_i + C \rightleftharpoons A_iC \tag{19}$$

In the case where components A and B are small molecules and component C is a polymer, Figure 1 shows a schematic representation of the species existing in solution. The equilibrium constants for the reactions (17)–(19) can be expressed as

$$K_{AA} = \frac{C_{A_{i+1}}}{C_{A_i}C_A}, \qquad K_{AB} = \frac{C_{A_iB}}{C_{A_i}C_B}, \qquad K_{AC} = \frac{C_{A_iC}}{C_{A_i}C_C} \tag{20}$$

In the infinite equilibria model for species A (eqs 17 and 20), the assumption is made that the equilibrium constant K_{AA} is the same for all dimer, trimer, and higher order i-mers formation.[47] In addition, a second assumption is made, related to the first, that the self-associating component A can form only linear associating species.[48]

The extent of hydrogen bonding for polymer sites C is given from the expression

$$\eta = \frac{C_{C_0} - C_C}{C_{C_0}} \tag{21}$$

The material balances for the three components, A, B, and C, are

$$C_{A_0} = \sum_{i=1}^{\infty} iC_{A_i} + \sum_{i=1}^{\infty} iC_{A_iB} + \sum_{i=1}^{\infty} iC_{A_iC} \tag{22}$$

$$C_{B_0} = C_B + \sum_{i=1}^{\infty} C_{A_iB} \tag{23}$$

$$C_{C_0} = C_C + \sum_{i=1}^{\infty} C_{A_iC} \tag{24}$$

By incorporating eqs 20 into eqs 22–24 and by taking into account that for any real number a, where $0 \le a \le 1$, the

following expressions are true

$$\sum_{i=1}^{\infty} a^i = a/(1-a)$$

$$\sum_{i=1}^{\infty} i a^i = a/(1-a)^2$$

equations 22–24 reduce to the expressions

$$C_{A_0} = \frac{C_A(1 + K_{AB}C_B + K_{AC}C_C)}{(1 - K_{AA}C_A)^2} \quad (25)$$

$$C_{B_0} = C_B\left(1 + \frac{K_{AB}C_A}{1 - K_{AA}C_A}\right) \quad (26)$$

$$C_{C_0} = C_C\left(1 + \frac{K_{AC}C_A}{1 - K_{AA}C_A}\right) \quad (27)$$

Equations 26 and 27 can be solved for C_B and C_C, respectively, and the resulting expressions are substituted back into eq 25 to obtain an algebraic expression for C_A. After tedious but straightforward algebra, the following fourth-order algebraic equation results

$$QC_A^4 + SC_A^3 + TC_A^2 + VC_A + Z = 0 \quad (28)$$

where

$$Q = K_{AA}^2(K_{AB} - K_{AA})(K_{AC} - K_{AA})C_{A_0} \quad (29)$$

$$S = (3K_{AA}K_{AB} + 3K_{AA}K_{AC} - 4K_{AA}^2 - 2K_{AB}K_{AC})K_{AA}C_{A_0} - (K_{AB} - K_{AA})(K_{AC} - K_{AA}) + K_{AA}K_{AB}(K_{AC} - K_{AA})C_{B_0} + K_{AA}K_{AC}(K_{AB} - K_{AA})C_{C_0} \quad (30)$$

$$T = (6K_{AA}^2 - 3K_{AA}K_{AB} - 3K_{AA}K_{AC} + K_{AB}K_{AC})C_{A_0} - (K_{AB} + K_{AC} - 2K_{AA}) - K_{AC}(K_{AB} - 2K_{AA})C_{C_0} - K_{AB}(K_{AC} - 2K_{AA})C_{B_0} \quad (31)$$

$$V = (K_{AB} + K_{AC} - 4K_{AA})C_{A_0} - K_{AB}C_{B_0} - K_{AC}C_{C_0} - 1 \quad (32)$$

$$Z = C_{A_0} \quad (33)$$

By substituting C_A back into eq 27, one obtains C_C and then from eq 21 η can be calculated.

Results and Discussion

For the systems examined, the hydrogen-bonding interactions were quantitatively determined and the resulting equilibrium constants are shown in Table II. $CHCl_3$ weakly self-associates forming dimers, and the equilibrium constant for this dimerization is approximately 2 orders of magnitude less than the other equilibrium constants.[19,20] As a result, the extent of self-association of $CHCl_3$ is small and so has little effect on the calculation of other equilibrium constants. Nevertheless, it should be taken into account in order to determine accurately the other equilibrium constants.

It should be noted that, for the CCl_4–$CHCl_3$–THF system, no specific interactions were observed between the acidic molecule of $CHCl_3$ and the basic molecule of THF. The characteristic absorption band of the O group of the cyclic ring of THF at 1070 cm^{-1} remains unchanged in shape and in intensity by the addition of different amounts of $CHCl_3$. It is possible that at that temperature the hydrogen bonding between the two components is very weak and/or the overlapping between the two peaks is very large.

In order to examine hydrogen bonding between components of moderate molecular size (components whose molecular weight is within the range 200–2000), the hydrogen-bonding interactions between tetraethylene glycol dimethyl ether (TGDE) and CH_3OH were examined. TGDE is a chain ether with five O groups per molecule capable of hydrogen bonding with molecules accepting electrons so that it can form one to five hydrogen bonds per molecule. In our approach, the probability that an O group will form a hydrogen bond is assumed to be independent of the other O groups. As a result, we can formulate a simple theory to take into account hydrogen-bonding interactions between TGDE molecules and other components of the system in terms of site–site interactions. We also assume that the segments of TGDE do not hydrogen bond with themselves. In the CCl_4–TGDE–CH_3OH system examined, the CH_3OH concentration was very low so that negligible self-association of methanol occurred. Addition of TGDE in the mixture results in hydrogen bonds between the O group of the TGDE and the OH group of methanol. In Figure 2, the characteristic absorption band of the methanol OH group at 3650 cm^{-1} is shown. In the absence of any TGDE in the mixture, no hydrogen bonding occurs so that only one peak is detected. By adding TGDE, a hydrogen-bonded peak appears at lower frequency as a result of the hydrogen bonding between CH_3OH and TGDE. This peak was not observed in a CCl_4–TGDE mixture. The hydrogen-bonding peak increases for higher TGDE concentration in the mixture. At the same time, the height and the area of the monomeric peak decrease because of the increasing number of CH_3OH molecules that hydrogen bond to TGDE sites. In Figure 3, the areas for the monomeric and the hydrogen-bonded peaks are shown as a function of the TGDE

Table II
Equilibrium Constants at 25 °C for the Systems Examined in This Work[a]

system	K, L/mol$_{seg}$	system	K, L/mol$_{seg}$
CH_3OH–CH_3OH	1.73	$CHCl_3$–PVMK	3.72
$CHCl_3$–$CHCl_3$	0.01	CH_3OH–PVMK	3.35
THF–CH_3OH	6.11	TGDE–CH_3OH	1.04

[a] The equilibrium constants for the self-association of methanol and chloroform were obtained from the literature.[17,19,20]

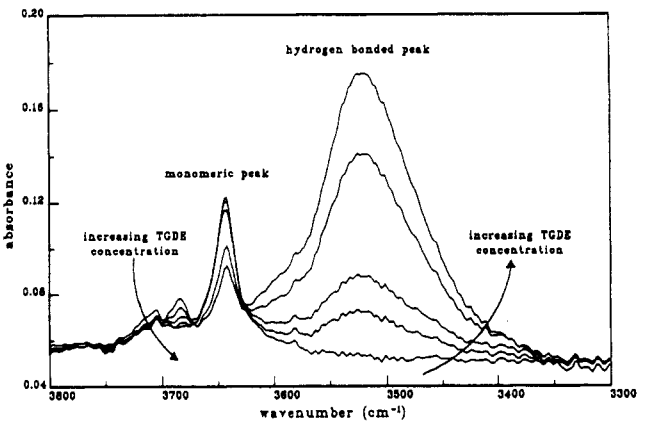

Figure 2. IR spectra of the system CCl_4–TGDE–CH_3OH in the region of the characteristic absorption band of CH_3OH at 3650 cm^{-1}. Without any TGDE in the mixture, there is only one peak at 3650 cm^{-1}, which corresponds to the monomeric CH_3OH molecules. As we add TGDE in the mixture, the height of this peak decreases whereas another peak at lower frequency appears. The new peak corresponds to the complex formation due to hydrogen bonding between TGDE and CH_3OH. The height of the new peak increases as the concentration of TGDE increases. In all the spectra, the concentration of CH_3OH was constant 0.03 mol/L and the different concentrations of TGDE were 0.0, 0.1135, 0.227, 0.908, and 1.589 mol$_{seg}$/L.

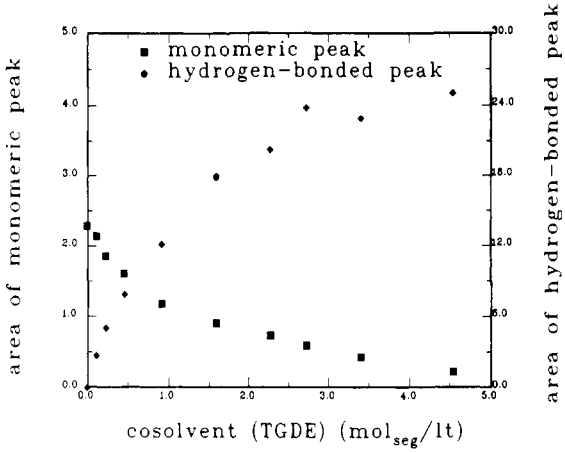

Figure 3. Areas under the two peaks of Figure 2 as a function of the TGDE concentration. As the concentration of TGDE in the mixture increases, the area of the monomeric peak decreases and the area under the hydrogen-bonded peak increases. In the case where no TGDE is in the mixture, the area of the hydrogen-bonded peak is zero.

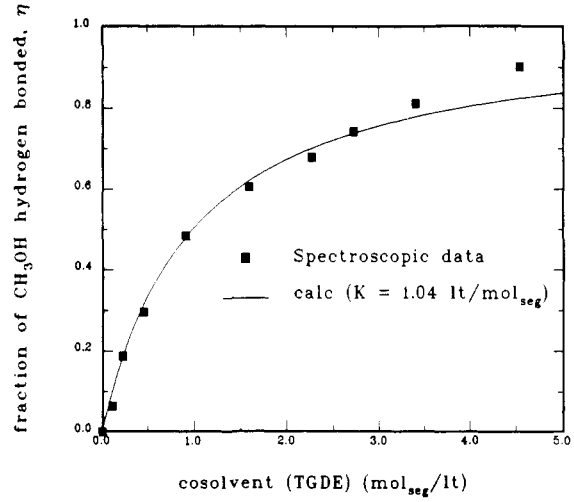

Figure 4. Spectroscopic data and calculations from chemical theory of the extent of hydrogen bonding, η, of CH_3OH as a function of the cosolvent, TGDE, concentration for the CCl_4–TGDE–CH_3OH mixture at 25 °C. The equilibrium constant is K = 1.04 L/mol$_{seg}$.

segment concentration. The areas were calculated by the technique described in detail in the Data Analysis section and in the Appendix. As the segment concentration of TGDE increases, the area of the monomeric peak decreases whereas the area of the hydrogen-bonding peak increases. From the areas of the monomeric peak the extent of hydrogen bonding of CH_3OH can be calculated. In Figure 4, the extent of hydrogen bonding for CH_3OH is plotted as a function of the TGDE segment concentration. The chemical theory calculations are in good agreement with the spectroscopic data, and this suggests that hydrogen bonding can be modeled for molecules of any size using this approach.

In Figure 5, the extent of hydrogen bonding of CH_3OH is shown as a function of the cosolvent concentration of THF. In the absence of any THF, all CH_3OH molecules are in the monomeric state since the CH_3OH concentration is extremely low to prevent self-association. Addition of THF to the mixture results in complex formation between CH_3OH and THF. When the THF concentration in the mixture is increased, the hydrogen bonding between CH_3OH and THF increases. Again, chemical theory calculations are in agreement with the experimental data.

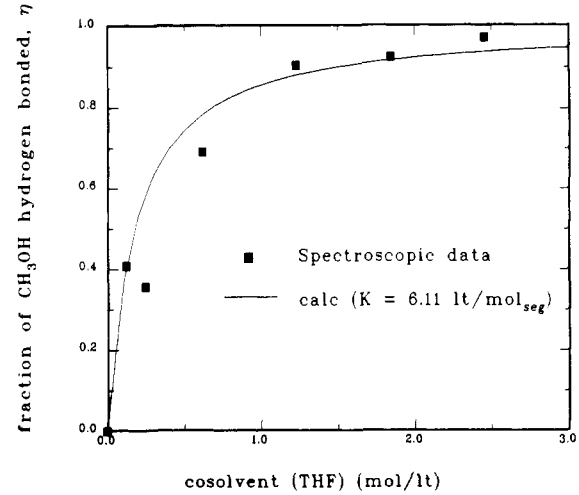

Figure 5. Spectroscopic data and calculations from chemical theory of the extent of hydrogen bonding, η, of CH_3OH as a function of the cosolvent, THF, concentration for the CCl_4–THF–CH_3OH mixture at 25 °C. The equilibrium constant is K = 6.11 L/mol.

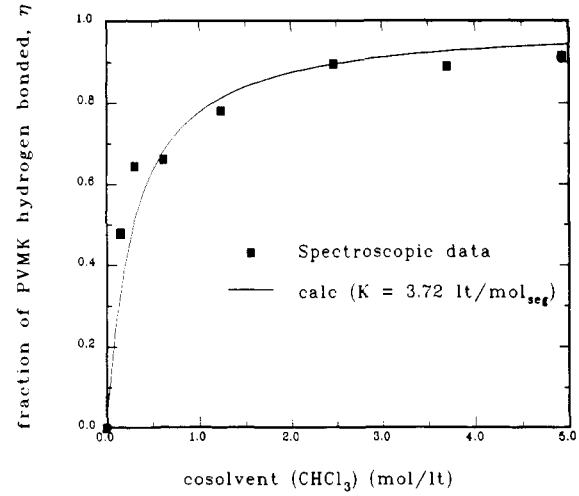

Figure 6. Spectroscopic data and calculations from chemical theory of the extent of hydrogen bonding, η, of PVMK as a function of the cosolvent, $CHCl_3$, concentration for the THF–$CHCl_3$–PVMK mixture at 25 °C. $CHCl_3$ dimerizes weakly. The solvation equilibrium constant is K = 3.72 L/mol$_{seg}$, and the $CHCl_3$ self-association equilibrium constant is K = 0.01 L/mol.

In Figure 6, the hydrogen-bonding interactions between PVMK and $CHCl_3$ are shown. In the absence of $CHCl_3$ from the system, no hydrogen bonding occurs between the basic sites of the polymer and the basic molecules of the solvent, THF. Addition of $CHCl_3$ results in complex formation between $CHCl_3$ and PVMK. In addition, $CHCl_3$ weakly self-associates forming dimers. However, no specific interactions between $CHCl_3$ and THF were observed as already explained. Again good agreement between chemical theory calculations and experimental results is obtained.

A ternary system was examined to test the competitive interactions between an amphoteric component (CH_3OH) and two basic components (THF and PVMK). In this system, the CH_3OH concentration varied from 0 to 10 mol/L so that self-association of CH_3OH must be taken into account. In addition, there were hydrogen-bonding interactions between CH_3OH and THF and between CH_3OH and PVMK. The absorption band of the C=O group of PVMK was examined to detect hydrogen-bonding interactions between CH_3OH and PVMK. The equilibrium constant for the CH_3OH self-association was obtained

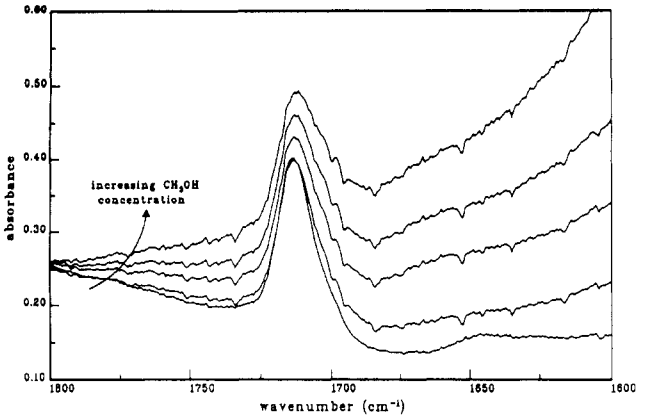

Figure 7. IR spectra for the mixture THF–CH_3OH–PVMK in the region near the characteristic absorption band of the C=O group of PVMK at 1713 cm^{-1}. The addition of CH_3OH results in complex formation between the CH_3OH molecules and the PVMK segments so that the C=O peak becomes broader and its height increases. Actually, there are two peaks (the monomeric peak and the hydrogen-bonded peak) in that region that are extremely overlapped. A Fourier self-deconvolution technique can partially resolve the two peaks. A characteristic absorption peak around 1510 cm^{-1} corresponding to the CH_3 group of CH_3OH affects the spectrum behavior at the region around 1713 cm^{-1} at high CH_3OH concentrations. The concentration of PVMK was constant, 0.03 mol_{seg}/L, in all the spectra whereas the CH_3OH concentrations were 0.0, 2.4694, 4.939, 7.408, and 9.878 mol/L.

from Walsh et al.[17] and the equilibrium constant for THF–CH_3OH was calculated before. In Figure 7, the characteristic absorption band of the C=O group of PVMK is shown for different CH_3OH concentrations. In the case where there is no CH_3OH in the mixture, only one peak is observed. Addition of CH_3OH results in a change in the shape and the height of the C=O peak. The peak becomes broader and its height increases. However, no clear distinction can be made between the monomeric peak and the hydrogen-bonding peak as was made for the OH peak of CH_3OH in Figure 2. In addition, there is a peak at lower frequency around 1510 cm^{-1} that corresponds to the CH_3 group of CH_3OH. As CH_3OH concentration increases, the height of this peak and the area under the peak increase. The tail of the CH_3 peak affects the spectrum behavior around the characteristic absorption band of the C=O group at 1713 cm^{-1}. By using the Fourier self-deconvolution technique described in the Appendix, it is possible to resolve partially the monomeric and the hydrogen-bonded peak. This technique in combination with a curve fitting of the raw data, the derivative of the data, and the Fourier self-deconvolution to the Voigt profile made possible the quantitative determination of the areas of the two peaks. In Figure 8, the spectrum for the mixture THF–CH_3OH–PVMK is shown in the region 1600–1800 cm^{-1}. The CH_3OH concentration was 9.878 mol/L. The fit using the nonlinear regression technique described in the Appendix also is shown. There is good quantitative agreement between the raw data and the curve fit. In Figure 8, the tail of the CH_3OH peak at 1510 cm^{-1} also is plotted, and it is shown that it has an appreciable effect in the region around the absorption band of the carbonyl group. The peaks corresponding to the nonbonded polymer sites and to the bonded polymer sites calculated with the technique described in the Appendix are plotted separately in Figure 8. The two peaks are within 8 cm^{-1} from one another and are overlapped. However, it is clear from Figure 8 that the technique used in this work is capable of resolving these types of peaks and so quantitative results can be obtained.

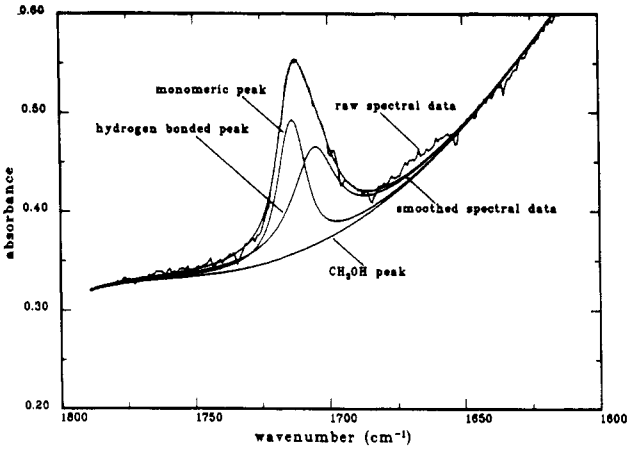

Figure 8. IR spectrum and the fit using the nonlinear regression technique described in the Appendix for the mixture THF–CH_3OH–PVMK in the region near the characteristic absorption band of the C=O group of PVMK at 1713 cm^{-1}. The PVMK concentration was 0.03 mol_{seg}/L and the CH_3OH concentration was 9.878 mol/L. The bottom line corresponds to the tail of the CH_3OH peak at 1510 cm^{-1} as calculated from the nonlinear regression technique. The calculated peaks corresponding to the nonbonded polymer sites at 1713 cm^{-1} and to the bonded polymer sites at 1705 cm^{-1} are plotted separately.

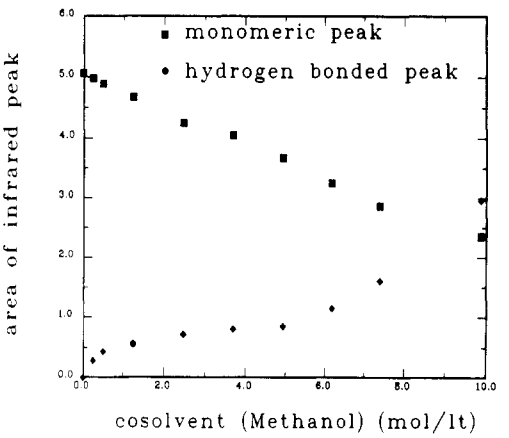

Figure 9. Areas under the two resolved peaks of Figure 8 as a function of the CH_3OH concentration. As the concentration of CH_3OH in the mixture increases, the area of the monomeric peak decreases and the area under the hydrogen-bonded peak increases. In the case where CH_3OH is absent from the mixture, the area of the hydrogen-bonded peak is zero.

In Figure 9, the areas of the monomeric and the hydrogen-bonded peaks are shown as functions of the CH_3OH concentration. From the areas of the monomeric peak the extent of hydrogen bonding of the PVMK sites is calculated and plotted in Figure 10 as a function of the CH_3OH concentration. The shape of the data for this system is qualitatively different from that of the other systems examined. It is interesting to note that the hydrogen bonding of the polymer increases linearly with the CH_3OH even though the interactions occurring in this system are more complicated than the interactions of the systems in Figures 4–6. The chemical theory calculations as discussed in the section "Chemical Theory for Polymer Systems" are in good agreement with the experimental data. One might think that it is easy to fit these data since there is an almost linear relation between the extent of hydrogen bonding of PVMK and the CH_3OH concentration. However, this is not the case. In Figure 10, calculations are shown ignoring the self-association of CH_3OH (dashed line) and ignoring both the self-association of CH_3OH and the CH_3OH–THF solvation. In the case where the CH_3OH self-association is ignored, predictions

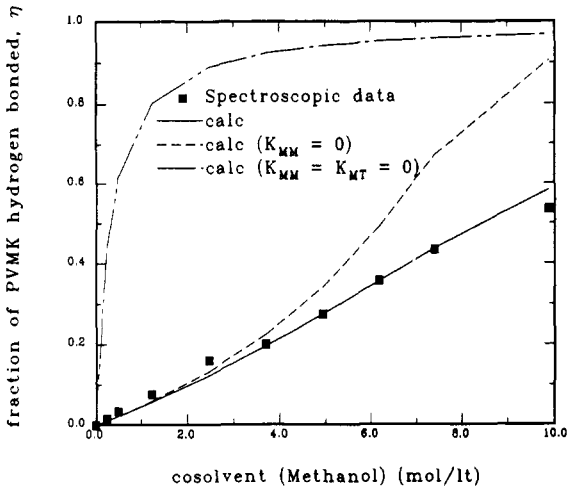

Figure 10. Spectroscopic data and calculations from chemical theory of the extent of hydrogen bonding, η, of PVMK as a function of the cosolvent, CH_3OH, concentration for the THF–CH_3OH–PVMK mixture at 25 °C (solid line). Notice the difference in the shape of the data from the data shown in Figures 4–6. In this system competitive hydrogen-bonding interactions exist between CH_3OH–PVMK and CH_3OH–THF. In addition, self-association of CH_3OH occurs. The equilibrium constants for these interactions are given in Table II. Calculations are shown ignoring the CH_3OH self-association (dashed line) and ignoring both the CH_3OH self-association and the CH_3OH–THF solvation.

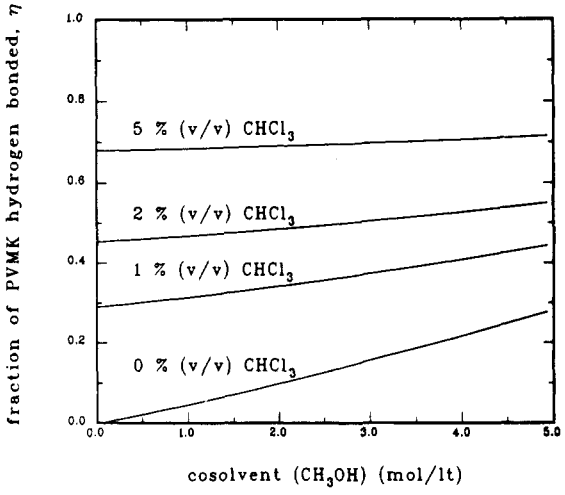

Figure 11. Calculations from chemical theory of the extent of hydrogen bonding, η, of PVMK as a function of the cosolvent, CH_3OH, concentration for the THF–$CHCl_3$–CH_3OH–PVMK mixture at 25 °C for different $CHCl_3$ concentrations. The equilibrium constants are obtained from the respective binary mixtures and are given in Table II.

are in agreement with the spectroscopic data only for low CH_3OH concentration. In addition, calculations considering only CH_3OH–PVMK interactions are very bad over the whole range of cosolvent concentration.

Using the spectroscopic data from the previous systems examined and the equilibrium constants for the hydrogen-bonding complexes calculated from chemical theory, we calculated the extent of hydrogen bonding of PVMK in a quaternary THF–$CHCl_3$–CH_3OH–PVMK mixture where the PVMK concentration was 0.03 mol_{seg}/L. In this system, PVMK hydrogen bonds to $CHCl_3$ and to CH_3OH whereas in the previous systems the solute hydrogen bonded to only one component. In Figure 11, η of PVMK is plotted as a function of the CH_3OH concentration for different $CHCl_3$ concentrations. In the absence of any $CHCl_3$ in the solution, the calculations are essentially the same as in Figure 10. By increasing the $CHCl_3$ and/or the CH_3OH concentration, the fraction of the polymer hydrogen bonded increases. However, the slope of η as a function of the CH_3OH concentration decreases for higher $CHCl_3$ concentration. When the volume fraction of $CHCl_3$ in the mixture is 5%, almost 70% of the polymer sites are hydrogen bonded. Addition of CH_3OH in the mixture has a negligible effect on the non-hydrogen-bonded polymer sites remaining in the mixture and so the slope of η as a function of CH_3OH concentration is almost zero.

Conclusions

We examined the hydrogen-bonding interactions between components of various molecular sizes. The density dependence of the hydrogen-bonding interactions between the different components seems to be independent of the molecular size of the components if the interactions are expressed in terms of segmental properties rather than molecular properties.

The approach used in this work to determine the intermolecular interactions between polymer molecules and small molecules can be used in the future to examine more complicated polymer molecules that exhibit both intermolecular and intramolecular interactions, for example, poly(ethylene glycol) and polyalcohols. In these systems more than one chemical equilibrium occurs.

Since good agreement between experimental data and the model's calculations were obtained, we believe that we can use the formulation described in this work to develop a more sophisticated theory to describe the thermodynamic properties of polymer solutions that hydrogen bond.

Acknowledgment. Support of this research by the Division of Chemical Sciences of the Office of Basic Energy Sciences, U.S. Department of Energy, under Contract No. DE-FG02-87ER13777 is gratefully acknowledged. We also acknowledge John Reilly for his suggestions in the data analysis.

Appendix

In this Appendix the nonlinear regression technique of Walsh et al.[16,17] using the Voigt profile for the spectral analysis is presented briefly. The Voigt profile is the convolution, or product in Fourier space, of the Lorentzian and Gaussian profiles and so accounts for all of the effects accounted for by these two profiles separately. The Voigt profile accounts for Doppler (Gaussian), natural (Lorentzian), and collision (Lorentzian) broadening of spectra.[49] Since the two profiles are combined through Fourier convolution, no additional parameters are introduced. The Voigt profile is characterized by height (h), peak position at maximum absorbance (ν_0), and the Gaussian (Doppler) (α_D) and Lorentzian (α_L) width parameters and is given by eq 2. By variation of the two width parameters (α_D, α_L) the Voigt profile makes a smooth transition between the pure Lorentzian and the pure Gaussian shapes. The main limitation of the Voigt profile over the Lorentzian profile is the excessive computation time needed to evaluate the convolution integral.[50]

There are two important aspects related to the accurate determination of monomeric and hydrogen-bonded species concentrations in solute–solvent mixtures. First is the accurate determination of peak areas and second is the accurate relation of areas to concentrations. The second aspect has been reviewed by Griffiths and de Haseth.[51] The area of each peak is determined by shape parameters that describe the spectra. These shape parameters are

again the height, peak position, and the half-breadth (half the width at half the height).

An important feature encountered with the monomeric and hydrogen-bonded carbonyl species is that they absorb at wavelengths close to each other and often the peaks partially overlap. The shape of each peak is affected since both peaks are influenced by the position and width of the other. If the spectral peaks (monomeric and hydrogen bonded) did not overlap, the area of each peak could be determined directly by integrating the spectrum. However, since the peaks do overlap, a method of separating them must be included in the data analysis. A reliable approach for the determination of areas of overlapped peaks is to use spectral analysis in combination with profile modeling. Recently, Jackson and Griffiths[52] and Walsh et al.[17] used a combination of Fourier self-deconvolution with profile modeling using the Lorentzian profile. Fourier self-deconvolution[21,51] is a technique used to narrow and therefore partially resolve overlapping peaks. For peaks that are only slightly overlapped either profile modeling or deconvolution can be used separately. The various merits of these two techniques have been discussed by many authors.[21,51,52] For peaks that are strongly overlapped neither technique is useful by itself and their combined application becomes necessary.

The spectra are analyzed by using derivatives and Fourier self-deconvolution to establish the number and position of peaks that are present (ν_0). Profile modeling then is used to determine the shape parameters (h, α_D, α_L) that characterize each peak in the spectrum. These shape parameters are determined not only by fitting the raw data but also by fitting the derivative and the Fourier self-deconvolution of the data. Fourier self-deconvolution improves the resolution of closely overlapped peaks,[21] while modeling the derivative improves the determination of shape parameters. The parameters obtained can be used to reproduce the spectra and therefore to accurately calculate the peak areas. The numerical method used to differentiate a spectrum is a three-point formula.[53] The major problem to be overcome in calculating the derivative of spectral data is that the derivative amplifies noise. In this work, derivatized data are smoothed using a "boxcar truncation" technique. The derivatized data are first converted to the Fourier domain using a fast Fourier transform.[54] Next, all frequencies greater than some optimal frequency are set equal to zero. Transformation back to the time domain results in a smooth curve. The optimal frequency is found by trial and error. A potential problem with this method is that the derivative can become distorted if the boxcar truncation eliminates an important part of the spectrum in addition to the noise. To avoid this, a comparison of the smoothed and original data should show that they have the same features.

Spectral analysis is displayed schematically in Figure 12, in which a simulated spectral curve is shown before and after differentiation and self-deconvolution. The first step in spectral analysis is to differentiate and self-deconvolute the raw spectral data. Each type of data (raw data, differentiated data, self-deconvoluted data) is then curve-fitted (modeled) using, respectively, the profile modeling function, the derivative of the profile modeling function, and the self-deconvolution of the modeling function. In general, slightly different sets of spectral parameters are obtained from modeling each type of data and an external optimization is used to find a single set of spectral parameters that gives the best overall fit. This is represented by the final spectrum in Figure 12. Using curve fits of the raw data, Fourier self-deconvolution, and

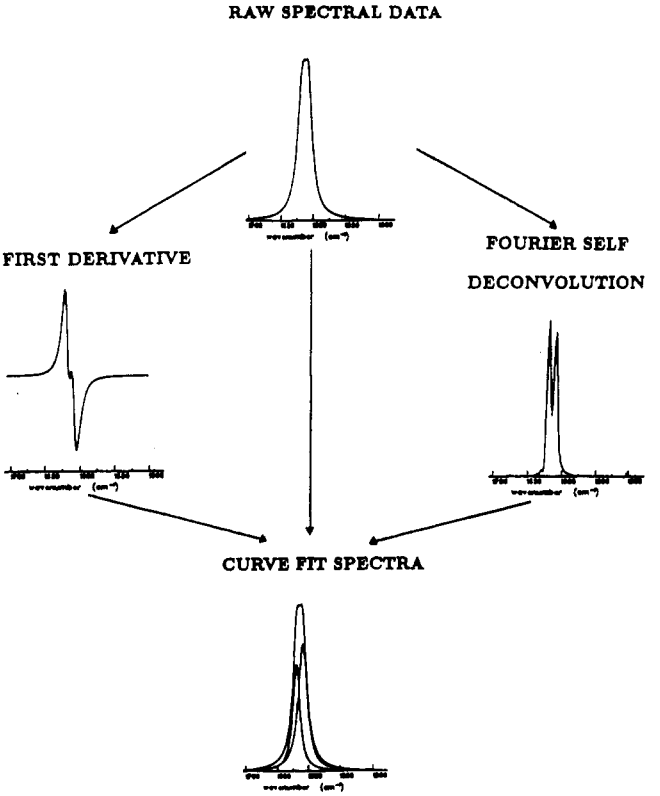

Figure 12. Schematic diagram of the spectral analysis technique described in the Appendix used to determine the area of the monomeric and hydrogen-bonded peaks. Nonlinear least-squares regression is applied to the spectral data, the Fourier self-deconvoluted spectral data, and the first derivative of the spectral data. The spectrum shown here is that of a simulated spectrum of two overlapping peaks.

first derivative, it is possible to obtain unique parameters that describe the individual peaks.

Finally, based on the characteristic parameters for the particular peak, the area under the peak is calculated by integrating the Voigt profile over all wavenumbers. The extent of hydrogen bonding is calculated based on the area of the monomeric peak according to the expression

$$\eta = (A_0 - A)/A_0 \qquad \text{(A1)}$$

where A_0 is the area of the monomeric peak when no hydrogen bonding is occurring and A is the area of the monomeric peak when hydrogen bonding is occurring.

References and Notes

(1) Philippova, O. E.; Kuchanov, S. I.; Topchieva, I. N.; Kabanov, V. A. *Macromolecules* **1985**, *18*, 1628.
(2) Coleman, M. M.; Moskala, E. J. *Polymer* **1983**, *24*, 251.
(3) Moskala, E. J.; Howe, S. E.; Painter, P. C.; Coleman, M. M. *Macromolecules* **1984**, *17*, 1671.
(4) Coleman, M. M.; Skrovanek, D. J.; Hu, J.; Painter, P. C. *Macromolecules* **1988**, *21*, 59.
(5) Lee, J. Y.; Painter, P. C.; Coleman, M. M. *Macromolecules* **1988**, *21*, 954.
(6) Skrovanek, D. J.; Howe, S. E.; Painter, P. C.; Coleman, M. M. *Macromolecules* **1985**, *18*, 1676.
(7) Skrovanek, D. J.; Painter, P. C.; Coleman, M. M. *Macromolecules* **1986**, *19*, 699.
(8) Musto, P.; Karasz, F. E.; MacKnight, W. J. *Polymer* **1989**, *30*, 1012.
(9) Allen, G.; Chai, Z.; Chong, C. L.; Higgins, J. S.; Tripathi, J. *Polymer* **1984**, *25*, 239.
(10) Albertsson, P. A. *Partition of Cell Particles and Macromolecules*, 3rd ed.; Wiley-Interscience: New York, 1986.
(11) Hefford, R. J. *Polymer* **1984**, *25*, 979.
(12) Haynes, C. A.; Beynon, R. A.; King, R. S.; Blanch, H. W.; Prausnitz, J. M. *J. Phys. Chem.* **1989**, *93*, 5612.
(13) Diamond, A. D.; Hsu, J. T. *AIChE J.* **1990**, *36*, 1017.

(14) Polik, W. F.; Burchard, W. *Macromolecules* **1983**, *16*, 978.
(15) Courval, G. J.; Gray, D. G. *Polymer* **1983**, *24*, 323.
(16) Walsh, J. M.; Reilly, J. T.; Greenfield, M. L.; Donohue, M. D. *Spectrochim. Acta*, in preparation.
(17) Walsh, J. M.; Greenfield, M. L.; Ikonomou, G. D.; Donohue, M. D. *Int. J. Thermophys.* **1990**, *11*, 119.
(18) Economou, I. G.; Ikonomou, G. D.; Vimalchand, P.; Donohue, M. D. *AIChE J.* **1990**, *36*, 1851.
(19) Green, R. D. *Hydrogen Bonding by C–H Groups*; Wiley: New York, 1974.
(20) Joesten, M. D.; Schaad, L. J. *Hydrogen Bonding*; Marcel Dekker Inc.: New York, 1974.
(21) Kauppinen, J. K.; Moffatt, D. J.; Mantsch, H. H.; Cameron, D. G. *App. Spectrosc.* **1981**, *35*, 271.
(22) Armstrong, B. H. *J. Quant. Spectrosc. Radiat. Transfer* **1967**, *7*, 61.
(23) Flory, P. J. *Principles of Polymer Chemistry*; Cornell University Press: Ithaca, NY, 1953.
(24) Prigogine, I. *The Molecular Theory of Solutions*; North Holland: Amsterdam, 1957.
(25) Flory, P. J. *J. Am. Chem. Soc.* **1965**, *87*, 1833.
(26) Beret, S.; Prausnitz, J. M. *Macromolecules* **1975**, *8*, 878.
(27) Sanchez, I. C.; Lacombe, R. H. *J. Phys. Chem.* **1976**, *80*, 2352.
(28) Donohue, M. D.; Prausnitz, J. M. *AIChE J.* **1978**, *24*, 849.
(29) Jin, G.; Walsh, J. M.; Donohue, M. D. *Fluid Phase Equilib.* **1986**, *31*, 123.
(30) Holten-Andersen, J.; Rasmussen, P.; Fredenslund, A. *Ind. Eng. Chem. Res.* **1987**, *26*, 1382.
(31) Flory, P. J. *J. Chem. Phys.* **1944**, *12*, 425.
(32) Acree, W. E. *Thermodynamic Properties of Nonelectrolyte Solutions*; Academic Press, Inc.: Orlando, FL, 1984.
(33) Tompa, H. *J. Chem. Phys.* **1953**, *21*, 250.
(34) Ginell, R.; Shurgan, J. *J. Chem. Phys.* **1953**, *23*, 964.
(35) Renon, H.; Prausnitz, J. M. *Chem. Eng. Sci.* **1967**, *22*, 299.
(36) Wiehe, I. A.; Bagley, E. B. *Ind. Eng. Chem. Fundam.* **1967**, *6*, 209.
(37) Renuncio, J. A. R.; Prausnitz, J. M. *Macromolecules* **1976**, *9*, 898.
(38) Panayiotou, C.; Vera, J. H. *Fluid Phase Equilib.* **1980**, *5*, 55.
(39) ten Brinke, G.; Karasz, F. E. *Macromolecules* **1984**, *17*, 815.
(40) Sanchez, I. C.; Balazs, A. C. *Macromolecules* **1989**, *22*, 2325.
(41) Prange, M. M.; Hooper, H. H.; Prausnitz, J. M. *AIChE J.* **1989**, *35*, 803.
(42) Painter, P. C.; Park, Y.; Coleman, M. M. *Macromolecules* **1988**, *21*, 66.
(43) Painter, P. C.; Park, Y.; Coleman, M. M. *Macromolecules* **1989**, *22*, 570.
(44) Painter, P. C.; Graf, J.; Coleman, M. M. *J. Chem. Phys.* **1990**, *92*, 6166.
(45) Painter, P. C.; Park, Y.; Coleman, M. M. *Macromolecules* **1989**, *22*, 580.
(46) Coleman, M. M.; Lichkus, A. M.; Painter, P. C. *Macromolecules* **1989**, *22*, 586.
(47) The assumption that the equilibrium constant is independent of the length of the i-mer is not correct for the alcohols, especially for the formation of the dimer. See, for example: Barker, J. *J. Chem. Phys.* **1952**, *20*, 794. Nevertheless, it is common to make this assumption[18,35,36] for simplicity.
(48) There is spectroscopic evidence that the alcohols form cyclic species in addition to the linear species. See, for example: Liddel, U.; Becker, E. D. *Spectrochim. Acta* **1957**, *10*, 70; Becker, E. D.; Liddel, U.; Shoolery, J. N. *J. Mol. Spectrosc.* **1958**, *2*, 1. However, the addition of another chemical equilibrium and subsequently another equilibrium constant will complicate further the problem and thus is avoided.
(49) Penner, S. S. *Quantitative Molecular Spectroscopy and Gas Emissivities*; Addison-Wesley Inc.: Reading, MA, 1959.
(50) Gabriel, C. J.; Mosier-Boss, P. A.; Szpak, S. *Spectrochim. Acta* **1987**, *43A*, 1293.
(51) Griffiths, P. R.; de Haseth, J. A. *Fourier Transform Infrared Spectrometry*; Wiley: New York, 1986.
(52) Jackson, R. S.; Griffiths, P. R.; Pierce, J. A.; Hongjin, G. *Proc. 7th Int. Conf. Fourier Transform Spectrosc. SPIE* **1989**, *1145*, 427.
(53) Abramowitz, M.; Stegun, I. *Handbook of Mathematical Functions with Formulas, Graphs and Mathematical Tables*; *NBS Appl. Math. Ser.* **1964**, *55*.
(54) Press, W. H.; Flannery, B. P.; Teukolsky, S. A.; Vetterling, W. T. *Numerical Recipes*; Cambridge University Press, Cambridge, 1986.

Registry No. PVMK, 25038-87-3; THF, 109-99-9; TBDE, 143-24-8; CCl_4, 56-23-5; $CHCl_3$, 67-66-3; CH_3OH, 67-56-1.